REPORT DOCUMENTATION PAGE

Form Approved
OMB No. 0704-0188

1. AGENCY USE ONLY (Leave blank)	2. REPORT DATE	3. REPORT TYPE AND DATES COVERED
		FINAL

4. TITLE AND SUBTITLE

1.3 Micrometer Fiber Photodetector

5. FUNDING NUMBERS

61102F
2301/AS

6. AUTHOR(S)

Professor Zhang

AFOSR-TR- 95 0159

7. PERFORMING ORGANIZATION NAME(S) AND ADDRESS(ES)

Rensselaer Polytechnic Institute
Troy, NY 12180-3590

8. PERFORMING ORGANIZATION REPORT NUMBER

9. SPONSORING/MONITORING AGENCY NAME(S) AND ADDRESS(ES)

AFOSR/NE
110 Duncan Avenue Suite B115
Bolling AFB DC 20332-0001

10. SPONSORING/MONITORING AGENCY REPORT NUMBER

F49620-93-1-0161

11. SUPPLEMENTARY NOTES

12a. DISTRIBUTION/AVAILABILITY STATEMENT

APPROVED FOR PUBLIC RELEASE: DISTRIBUTION UNLIMITED

12b. DISTRIBUTION CODE

13. ABSTRACT (Maximum 200 words)

Under the support from AFOSR, we have studied ultrafast optoelectronics in two projects: (1) time-resolved optoelectronic measurements of nitrogen-implanted GaAs crystals and InGaAs; and (2) photoreponse of Si/Ge superlattice and its alloy materials.

~~SEE ATTACHED ABSTRACT~~

14. SUBJECT TERMS

15. NUMBER OF PAGES

16. PRICE CODE

17. SECURITY CLASSIFICATION OF REPORT	18. SECURITY CLASSIFICATION OF THIS PAGE	19. SECURITY CLASSIFICATION OF ABSTRACT	20. LIMITATION OF ABSTRACT
UNCLASSIFIED	UNCLASSIFIED	UNCLASSIFIED	UNCLASSIFIED

AFOSR Final Technical Report (F49620-93-1-0161)

Submit to:

Dr. Schlossberg
AFOSR
Bolling Air Force Base
Washington DC 20332-6448

Prepared by:

X.-C. Zhang,

Physics Department
Rensselaer Polytechnic Institute
Troy, NY 12180-3590 USA
Tel: (518) 276-3079
Fax: (518) 276-6680

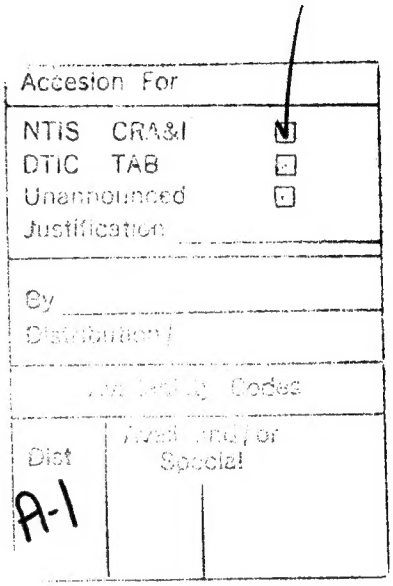

Abstract

Under the support from AFOSR, we have studied ultrafast optoelectronics in two projects: [1] time-resolved optoelectronic measurements of nitrogen-implanted GaAs crystals and InGaAs; and [2] photoresponse of Si/Ge superlattice and its alloy materials.

Results from AFOSR Support

AFOSR Award:

Award number F49620-93-1-0161, $24,983

Publication and submission supported in part by the award:

1 Y. Jin, D.F. Liu, G.A. Wagoner, W.D. Phillips, T. Sangsari, J. Perkin, M. Alexander, X.-C. Zhang, "Temperature Dependence of THz Emission from <111> GaAs via Trans-Resonant Excitation," Submitted to Appl. Phys. Lett. (1994)

2 X.-C. Zhang and Y. Jin, "Generation of THz Radiation from Semiconductors," submitted to Ultra-Wideband, short-Pulse Electromagnetics, Ed. by Carin, Plenum Press, (1994)

3 Y. Jin, X.F. Ma, G.A. Wagoner, M. Alexander, X.-C. Zhang, "Anomalous Optically Generated THz Beams from Metal/GaAs Interfaces," Appl. Phys. Lett., **65**, 682 (1994)

4 X.-C. Zhang, Y. Jin, X.-F. Ma, A. Rice, K. Ware, D. Bliss, J. Perkin, M. Alexander, "Sum-Frequency Generation and Difference-Frequency Generation near Bandgap of Zincblende Crystals," Appl. Phys. Lett., **64**, 622 (1994)

5 A. Rice, Y. Jin, X.-F. Ma, X.-C. Zhang, D. Bliss, J. Perkin, M. Alexander, "Terahertz Optical Rectification from <110> Zincblende Crystals," Appl. Phys. Lett., **64**, 1324 (1994)

6 S. Hong, Y. Jin, G. Wagoner, X.-C. Zhang, L. Kingsley, "Time-Resolved Optoelectronic Measurements of Nitrogen-implanted GaAs Crystals," Ultrafast Phenomena, **7** (1994)

7 X.-C. Zhang, "New Terahertz Sources and Applications," IEEE/LEOS News Letter, **7-4**, 14 (1993)

8 X.F. Ma and X.-C. Zhang, "Determination of Ratios Between Nonlinear Optical Coefficients by Using Subpicosecond Optical Rectification," JOSA B, **10**, 1175 (1993)

9 X.-C. Zhang, T.-M. Lu, C. P. Yakymyshyn, "Intense THz Beam from Organic Electro-Optic Materials," Ultrafast Electronics and Optoelectronics, **14**, 119 (1993)

[1] Time-Resolved Measurements of Nitrogen-Implanted GaAs Crystals

We compared the measurement of optically induced THz radiation and time-resolved photoreflectance ($\Delta R/R$) from nitrogen-ion implanted GaAs samples, where surface implantation densities ranged from $1x10^8$ cm^{-2} to $5x10^{15}$ cm^{-2}.

Understanding the effects of electrochemical passivation on the electronic properties of semiconductor surface states is crucial to semiconductor device fabrication. Previous results indicated that the static electric field across the surface of a semiconductor is substantially modified by hydrogen plasma passivation. As an example, after 30 minutes of passivation, the surface field from n(p)-type GaAs samples has been shown to increase by up to a factor of 2(10). Herein, we report the results of our recent measurements of the transient optoelectronic properties of nitrogen-ion implanted GaAs, where the nitrogen ions served as isoelectronic centers and surface implantation densities ranged from $1x10^8$ cm^{-2} to $5x10^{15}$ cm^{-2}. Optically induced THz electromagnetic radiation and time-resolved photoreflectance ($\Delta R/R$) measurements were made and the results of these two different optoelectronic techniques was compared. Both measurements show strong dependence on implantation density and either technique is a good diagnostic of surface implantation density.

GaAs substrates were cleaved from a single semi-insulating GaAs wafer. The measured resistivity and steady state mobility were over 10^7 Ω·cm and 4,000 $cm^2 \cdot V^{-1} \cdot s^{-1}$, respectively. The substrates were then implanted with nitrogen ions. One GaAs substrate remained unimplanted and served as a reference sample. The implantation was performed on a Varian 350R Medium-Energy & Medium-Current ion implanter. The beam current ranged from 0.18 μA to 100 μA, increasing proportionally with dose level. The typical sample temperature was kept below 80 °C and no annealing was performed after ion-implantation. The energy of the incident nitrogen ions was set at 180 keV. Nitrogen ion surface densities ranged from $1x10^8$ cm^{-2} to $5x10^{15}$ cm^{-2}, with incremental steps alternating between a factor of 2 and 5 successively. The mean value of the damage depth in the samples was approximately 0.6 μm which is comparable to the optical absorption length (α^{-1} = 0.7 μm at λ = 810 nm).

The optical source was a mode-locked Ti:sapphire laser, operating at a central wavelength of 810 nm. During the measurement of optically-induced THz radiation emitted from the wafers, the waist of the normally-incident, unfocused optical beam was approximately 4 mm. Further, the wafers were subjected to an external magnetic field of roughly 0.3 Tesla, which was perpendicular to the direction of optical propagation and was applied via pair of permanent magnets. The forward THz radiation was detected by an ultrafast photoconducting antenna. In the time-resolved photoreflectance experiment (pump / probe), the laser beam was focused to spot size of approximately 100 μm. Both experiments were performed at room temperature.

Because the unimplanted GaAs wafer was slightly n-type, the direction of its surface depletion field was outward. However, since nitrogen ions are an isoelectronic element for GaAs, after implantation, the field direction reversed. The THz radiation waveforms emitted from a GaAs wafer prior to, and after implantation at $5x10^{11}$ cm^{-2} are shown in Fig. 1. The observed polarity flip is associated with a reversal in the direction of the surface depletion field. Fig. 2 displays THz radiation waveforms from several ion-implanted samples with implantation surface densities ranging from $5x10^{11}$ cm^{-2} to $5x10^{14}$ cm^{-2}.

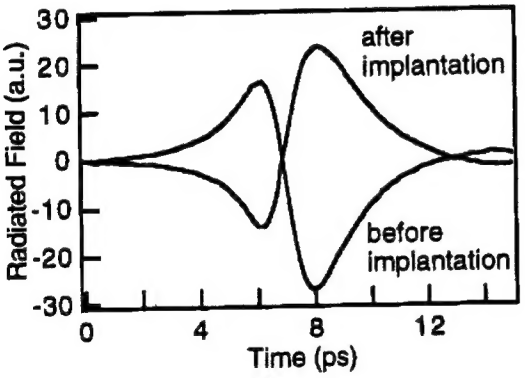

Fig. 1

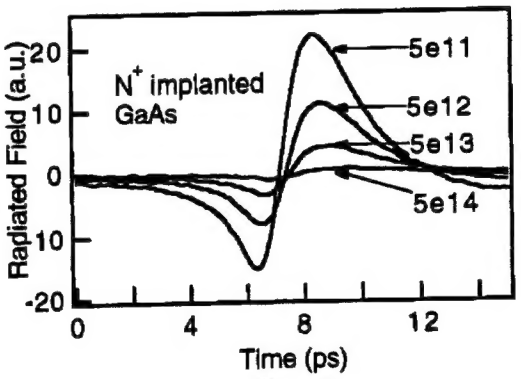

Fig. 2

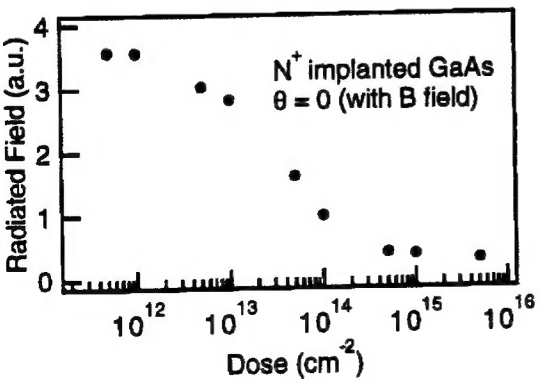

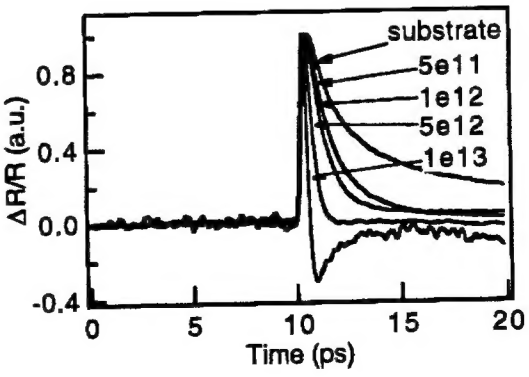

Fig. 3 Fig. 4

Fig. 3 plots the amplitude of THz radiation versus ion dose level. THz signal decreases as surface implantation density increases. Fig. 4 shows normalized temporal waveforms of modulated photoreflectance signals, ($\Delta R/R$) from both implanted and unimplanted samples. Corresponding with increased implantation density, is a significant decrease in the $\Delta R/R$ waveform decay time. For samples with ion dose levels greater than $1x10^{13}$ cm^{-2}, decay times as short as 0.35 ps have been observed. Fig. 5 plots the peak values of the photoreflectance signal versus implant density. From samples with implant densities greater than 10^{14} cm^{-2}, we observe a sign change in the peak value of the photoreflectance signal.

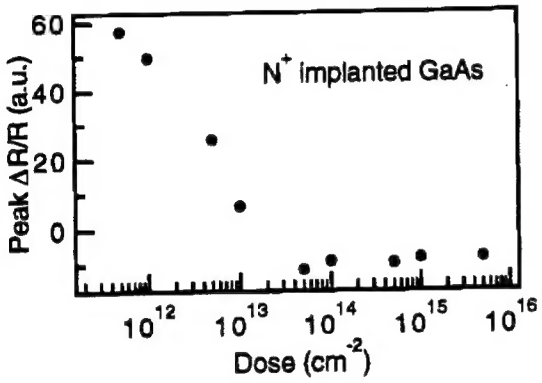

Fig. 5

In summary, we report the measurement and comparison of optically induced THz radiation and time-resolved photoreflectance from nitrogen-ion implanted GaAs samples.

Currently, we are studying the possibility to switch large photocurrent (up to kA) in the THz photoconducting antennas, which is in impractical with conventional contacting methods. We believe that the remote magnetic control to the intense THz radiation has the potential to be used in THz beam steering system. We also established the sample exchange program with Raytheon. Now we can get InGaAs samples (both bulk and MBE growth samples) from them. We have measured over 9 different low temperature InGaAs samples sets (alloyed and superlattice samples). Our measurement shows 7.1 to 24 ps carrier lifetime of their low temperature InGaAs. These materials are grown for 1.3 μm detectors.

SI/Ge Auston Switches:

We have designed and fabricated a mask for ultrafast optoelectronic measurement, including carrier lifetime measurement of SiGe materials. The pattern of the mask is shown in Figure 6. This mask has been used to make many antenna structures for several scientists in Air Force Base (Dr. Sam Howelis, Kirtland AFB, and Dr. M. Alexander) and Army Research Office (Dr. B. Guenther).

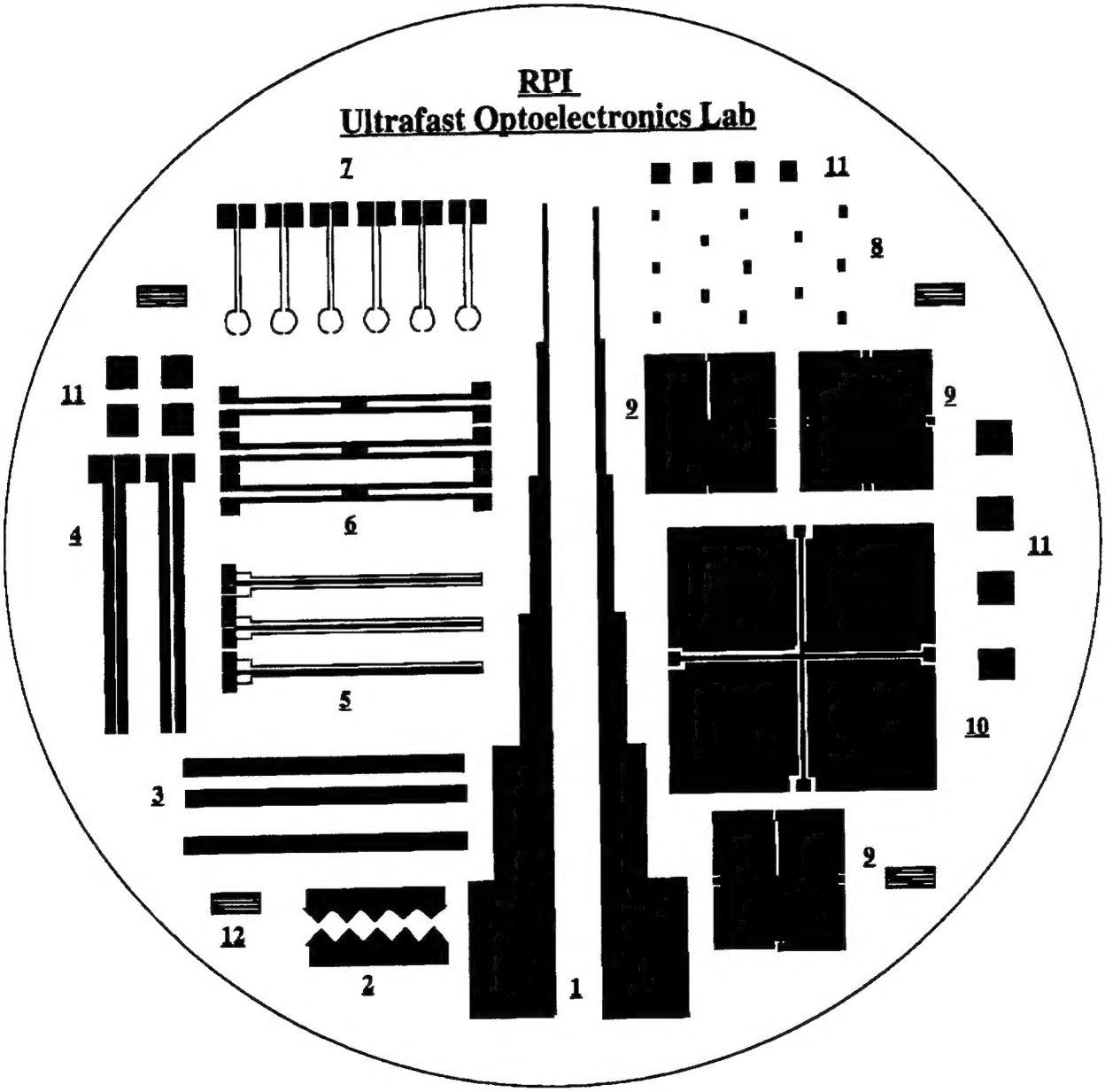

Structure Description

1. Step electrodes (1)

Step height	1 cm
Step number	6
Electrode width	5, 10, 50, 500, 2000, 5000 μm
Gap width	4 mm

2. Zig-zag array (1)

Length	1 cm
Electrode width	0.5 mm
Zig height	1 mm
Small gap	0.1 mm

3. Large electrode set (2)

Length	2 cm
Electrode width	2 mm
Gaps	2, 4 mm

4. Small electrode set (2)

Pads	1 mm by 1.5 mm
Wire width	1 mm
Gaps	50, 100 μm

5. Double antenna (3)

Electrode pads	1 mm by 1 mm
Wire	10 μm
Separation	5 μm
Top widths	50, 100, 200 μm

6. Dipole antenna (3)

Electrode pads	1 mm by 1 mm
Length	2 cm
Small gap	5 μm
Separation	50, 100, 200 μm

7. Magnetic field sensors (6)

Electrode pads	1 mm by 1 mm
Overall length	1 cm
Wire width	10 μm
Separation	10 μm
Loop radius	50, 100 μm
Opening	none, 5 μm, 10 μm

8. Square dot detectors (2 x 5)

Side length	100 μm and 200 μm
Gaps	2, 3, 4, 5 10 μm
Distance	5 mm

9. Small Auston switch (3)

Size	1 cm by 1 cm
Wire	10 μm
Gap	10 μm
Wire	10 μm
Gap	5 μm
Wire	5 μm
Gap	2 μm

10. Large Auston switch (1)

Size	2 cm by 2 cm
Wire	10 μm
Gap	5 μm

11. Electrode pads
2 mm by 2 mm, 1 mm by 1 mm

12. Manufacture aids: line pair

Width	2 μm
Separations	2 μm
Number	20

We have fabricated two Auston switches on Si/Ge superlattice samples. The materials was provided by IBM T.J. Watson Research Center. We sent the samples out for ion implantation. We have test them using 820 nm laser pulse (Ti:sapphire laser). The test indicated the structures were good. 2 to 5 picosecond photoresponses have been achieved. However, at 1.3 μm (measurement done by Dr. Ray Boncek at Rome Lab.), one sample showed no photoresponse and other has a small photoresponse. A SiGe alloy sample shows a better photoconductivity. Recently IBM donated their Si/Ge MBE to Prof. W.I. Wang (Columbia Univ.), so we can not get samples from them within a short time. Currently we are contacting with AT&T Bell Laboratory for new MBE materials, and IBM for MOCVD growth materials.

For the first time, we achieved photocurrent in our magnetic field sensor which is our item 7. These sensors are current loops. The material for photoconductor is LT GaAs. We are able to measure picosecond magnetic pulses. Our signal to noise is better than 150 with a 300 ms of lock-in amplifier integration time.